ACS OMEGA

Open Access

http://pubs.acs.org/journal/acsodf

Article

Empowering an Acute Kidney Injury 3D Graphene-Based Sensor Using Extreme Learning Machine

Netnapa Sittihakote, Pobporn Danvirutai, Sirirat Anutrakulchai, Adisorn Tuantranont, and Chavis Srichan*

Cite This: *ACS Omega* 2024, 9, 21276−21286

Read Online

ACCESS | Metrics & More | Article Recommendations

ABSTRACT: This study reports on the application of an extreme learning machine (ELM) in near-real-time kidney monitoring via urine neutrophil gelatinase-associated lipocalin (NGAL) detection with a 3D graphene electrode. This integration marks the first instance of combining a graphene-based electrode with machine learning to enhance the NGAL detection accuracy, building on our group's 2020 research. The methodology involves two key components: a graphene electrode functionalized with a lipocalin-2 antibody for NGAL detection and the ELM application for improved prediction accuracy by using urine analysis data. The results show a significant 15% increase in the area under the curve (AUC) for NGAL determination, with error reduction from ±6 to 0.54 ng/mL within a linear range of 2.7−140 ng/mL. The ELM also lowered the detection limit from 14.8 to 0.89 ng/mL and increased accuracy, precision, sensitivity, specificity, and F1 score for AKI prediction by 8.89, 30.69, 6.78, 9.94, and 19.07%, respectively. These findings underscore the efficacy of simple neural networks in enhancing graphene-based electrochemical sensors for AKI biomarkers. ELM was chosen for its optimal performance-resource balance, with a comparative analysis of ELM, support vector machines, multilayer perceptron, and random forest algorithms also included. This research suggests the potential for miniaturizing AI-enhanced sensors for practical applications.

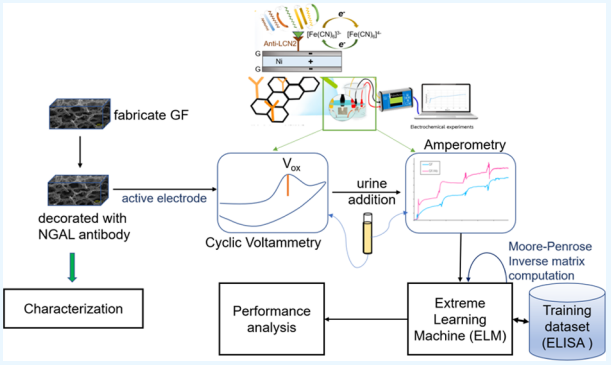

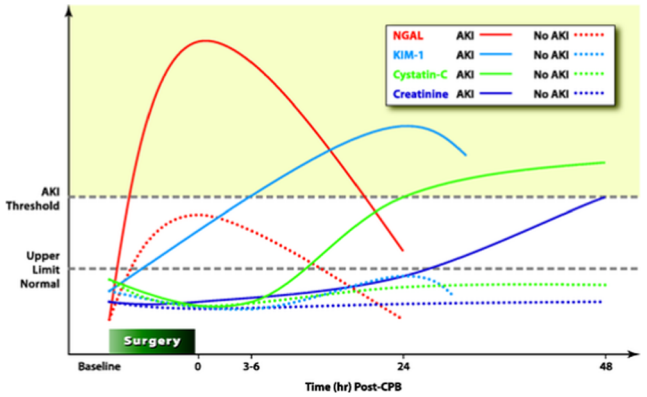

Figure 1. Response time of AKI biomarkers: monitored after surgery: creatinine, Kim-1, cystatin C, and NGAL. During and after surgery before AKI occurred, these biomarkers were plotted over time. NGAL showed the fastest response time, rising to the peak within 2 h. Reprinted with permission from The Journal of the American Society of Anesthesiologists, 2010 Apr 1;112(4):998−1004. Copyright 2010, Wolters Kluwer Health, Inc.[8]

1. INTRODUCTION

Acute kidney injury (AKI) stands as a critical global health concern, which may arise without notice if no specific sensors are applied. Unfortunately, despite over 50 years, the comorbidity rates of AKI have shown no improvement. The presence of AKI significantly elevates the risk of heart failure by 58%, myocardial infarction by 40%, and stroke by 15%.[1] Particularly prevalent in hospitals in high-income countries (HICs), AKI predominantly affects elderly patients with underlying conditions and those undergoing procedures like renal dialysis, often induced by iatrogenic factors such as surgical interventions and healthcare-associated infections. Conversely, in low-to-middle-income nations (LMICs), AKI occurs more frequently outside hospitals and is linked to various factors, including infections, dehydration, electrolyte imbalances, toxic ingestion, and pregnancy-related complica-

Received: February 12, 2024
Revised: April 18, 2024
Accepted: April 23, 2024
Published: May 1, 2024

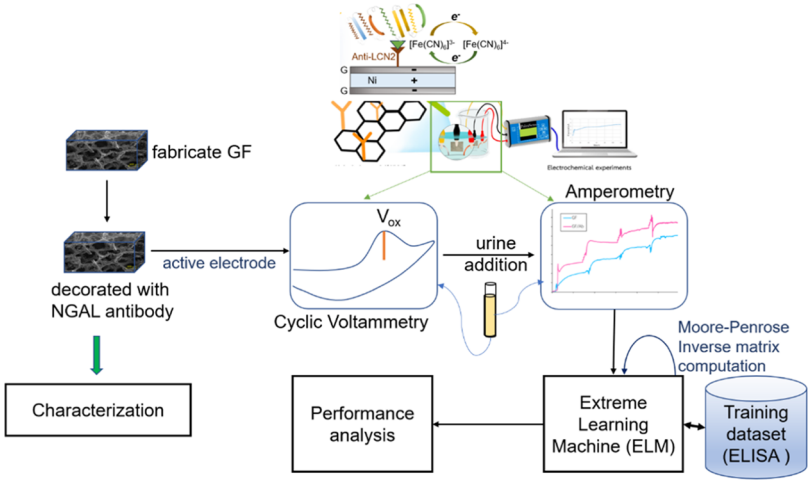

Figure 2. Overall picture from nanomaterials based on microporous graphene, electrode functioning, and embedding a machine learning model (ELM) for performance improvement.

tions. Notably, AKI in LMICs tends to impact a younger demographic compared to HICs. AKI manifests as a condition marked by a sudden decline in glomerular filtration rate (GFR), impacting toxin removal capability and attributing to several morbidity factors.[1] Neutrophil gelatinase-associated lipocalin (NGAL) biomarker arises as one of the most rapid responses addressing the occurrence of AKI.[2−4]

The Kidney Disease Improving Global Outcome (KDIGO) criteria for diagnosing acute kidney injury (AKI), established in 2012, relies on increased serum creatinine (SCr) levels and altered urine output.[3] However, SCr's delayed responsiveness, often taking up to 72 h to reflect acute renal injury, limits its practicality for real-time monitoring. Consequently, alternative biomarkers such as kidney injury molecule-1 (Kim-1), cystatin C, and NGAL have gained prominence. Notably, NGAL emerges as a promising candidate for early diagnosis, exhibiting rapid responsiveness within 2 h to renal injury. A comparison of the response times of different biomarkers upon kidney injury is illustrated in Figure 1. We selected NGAL as the AKI biomarker for its fastest response time (within 2−24 h). Kim-1, cystatin C, and creatinine response to AKI were 6 h, 34 h, and 48 h, respectively.[5−9]

Originating from the bone marrow during myeloid leukocytosis and stored in neutrophils, NGAL is predominantly released by the loop of Henle and associated tubules in cases of renal tubular epithelial cell damage, positioning it as an early predictive biomarker for kidney dysfunction. The 25 kDa NGAL is secreted and elevated in serum and urine, correlating with acute renal failure and offering the potential for timely assessment of damage severity. This stresses NGAL's significance in advancing both the diagnosis and prognosis of chronic kidney disease (CKD) and facilitating the evaluation of treatment efficacy.[6]

Various methodologies, such as plasma-based fluorescence immunoassay,[2] urine sample immunoblotting,[10] enzyme-linked immunosorbent assay (ELISA), and chemiluminescent magnetic immunoassay (CMIA) with healthy urine,[11] have been employed for quantifying NGAL. However, these methods involve high costs and lengthy processing times. Electrochemical methods, especially with downscaled working electrodes, are widely used for label-free and portable biosensing devices. Despite the advantages, downsizing the working electrode may compromise the sensor surface area and sensitivity to be reduced compared to that of a large-electrode device. Utilizing graphene-based electrodes could greatly enlarge the reactive surface of a miniaturized electrode. Graphene offers an extraordinarily high surface area per mass, thereby enhancing the sensitivity and resolving the mentioned issues. Among graphene electrodes, 3D-folded graphene or graphene foam (GF) possesses a greater reactive surface per unit volume compared to flat graphene.

In the literature, modifications to the working electrode were proposed to enhance the sensitivity and specificity of electrochemical sensors. Various electrode morphologies have been proposed for specifically detecting NGAL. For instance, an ITO/TiO2/CoPc/CS/SA/BSA/BiNb/NGAL sensor, utilizing a photoelectron-chemical transduction technique, was employed for serum NGAL detection.[12] Additionally, an electrochemical aptasensor using GSPE/P(ATT)-GO/AuNPs/Apt1/LCN2/Apt2 electrodes was developed for NGAL detection in fetal bovine serum through DPV signal analysis.[13] Carbon/enzyme-based configurations are utilized for serum sample analysis employing cyclic voltammetry (CV).[14] Among various alterations of potential or current in electrochemical measurements, CV is particularly crucial as it can determine the reduction and oxidation potentials, along with the redox current correlated to the analyte concentration. Following the determination of redox potentials by CV, chronoamperometry is applied for fast detection and to enable a miniaturized detection device for the analyte.

Graphene, a single-atom-thick carbon material, exhibits exceptionally high electron mobility, with the electron velocity in graphene reaching 1/300 compared to the velocity of light. With an extraordinarily high reactive surface area of 2.1×10^7 cm^2/g, graphene stands out as a distinctive candidate for sensing materials. The 3D folding of graphene on a microporous scaffold further amplifies the surface area per unit volume compared to that of a single flat graphene sheet. This ongoing research in NGAL detection builds upon our previous work,[15] involving the collection and testing of real human urine samples, along with the incorporation of neural networks for performance enhancement, as reported in this article.

Xiao et al. (2022) reviewed the artificial intelligence (AI) applications focused on AKI, highlighting various approaches for predicting AKI prognosis.[16] While numerous AI methods

https://doi.org/10.1021/acsomega.4c01315
ACS Omega 2024, 9, 21276−21286

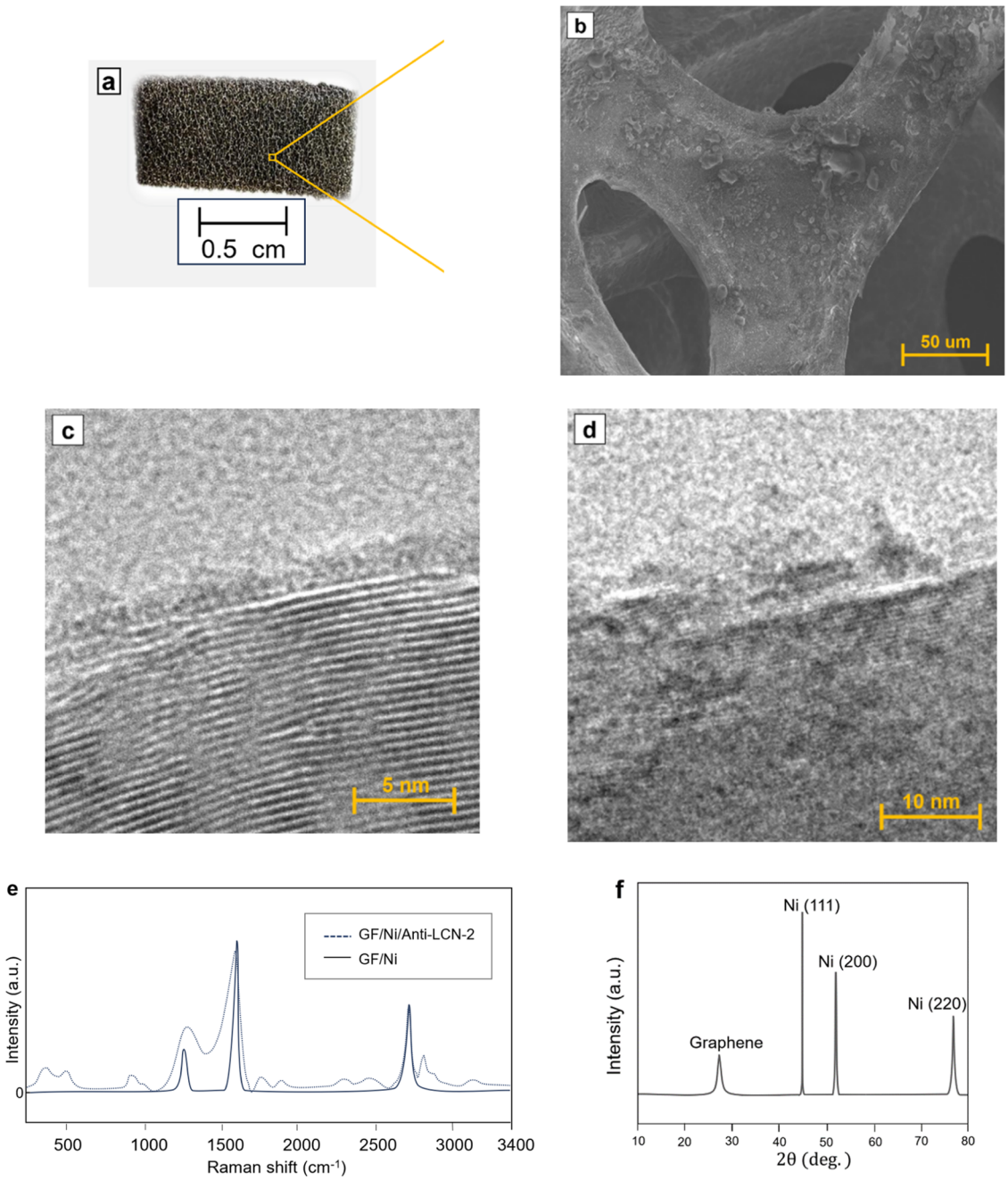

Figure 3. GF characterization via (a) visible-light image, (b) FE-SEM, (c) HR-TEM, and (d) BF-TEM. HR-TEM and BF-TEM display the existence of graphene layers in GF. (e) Raman spectra with and without antibody conjugation (noise filtering applied). (f) XRD pattern of the GF.

exist for this purpose, limited attention has been given to AI-powered AKI biomarker determinations. This study aims to demonstrate the efficacy of the simplest neural network or extreme learning machine (ELM) in enhancing electrochemical determination. Before selecting ELM for further investigation, a comparative analysis is conducted with other machine learning models, including support vector machines (SVMs), multilayer perceptrons (MLPs), and random forest (RF) algorithms. The work contributes by reporting the first application of ELM in the electrochemical prediction of NGAL with a graphene-based electrode. Performances of pure GF/Ni/Anti-LCN2 and the electrode with ELM were compared in terms of AUC and error improvement for AKI discrimination. Incorporating machine learning into NGAL prediction serves to eliminate nonzero interference factors present in human urine, such as electrolytes and albumin. The comprehensive overview of this research is illustrated in Figure 2.

2. MATERIALS AND METHODS

This section will start with electrode material fabrication, beginning with details on the electrochemical setup and measurements and electrode fabrication. The second part contains performance improvement using ELM. Overall methods can be illustrated in Figures 2 and 4. Characterization equipment included a field-emission scanning electron microscope (FE-SEM: Hitachi, SU-8030), a high-resolution tunneling electron microscope (HR-TEM: JEOL, JEM-2010), bright-field tunneling electron microscope (BR-TEM:

https://doi.org/10.1021/acsomega.4c01315
ACS Omega 2024, 9, 21276−21286

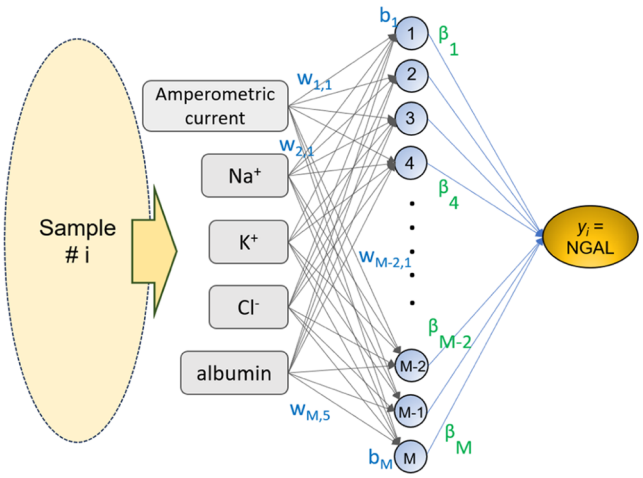

Figure 4. ELM is used for performance improvement after pure electrochemical measures.

Table 1. Distribution of the Data Set Used to Train ELM for NGAL Predictions[a]

	N	minimum	maximum	mean	SD
creatinine (mg/dL)	135	26.2	114	55.2	34.9
protein (mg/dL)	135	91.0	785	351	294
albumin (mg/dL)	135	620	2268	1193	699
Na^+ (mmol/L)	135	10.0	49.0	30.8	13.9
K^+ (mmol/L)	135	5.00	21.2	10.8	6.25
Cl^- (mmol/L)	135	9.00	33.0	20.4	8.76
valid N (listwise)	135				

[a]Results were obtained from urine analysis of the 135 samples.

Table 2. Patient Characteristics and Clinical Outcomes

parameter	case
total	135
male:female	60:75
requiring kidney replacement therapy (KRT)	36
nephrotic syndrome	24
chronic kidney disease	19
diabetes mellitus	13
hypertension disease	10
dyslipidemia	6
others	27

JEOL, JEM-2010), and X-ray diffraction (XRD: Rigaku, TTRAXIII) using Cu Kα radiation (30 kV, 15 mA) at a detection speed of 3°/min, and a confocal Raman spectrometer (Horiba XploRA PLUS, Horiba Jobin Yvon, Northampton, U.K.) with a 50× objective lens (LMPLFL50X, Olympus, St. Joseph, MI). The characterizations are shown in Figure 3. The diagram of the extreme learning machine for accuracy improvement of NGAL prediction is shown in Figure 4.

2.1. Electrode Fabrication. An active electrode in this study was composed of 3D microporous graphene with lipocalin-2 (LCN2) antibody functionalized on its surface. GF was fabricated using chemical vapor deposition (CVD) with Ni foam as the catalyst. Ni foam was placed inside a (1 Torr) vacuum furnace tube aligned horizontally. The tube was heated up to 900 °C with C_2H_2 flowing into the tube. After heating, the tube underwent rapid cooling (15 °C/min). This yields carbon atoms deposited as a graphene surface on the foam scaffold. After the cooling process, nickel was partially etched by a 3 M HCl solution at 60 °C for 30 min. FE-SEM, HR-TEM, BF-TEM, Raman, and XRD of the GF are shown in Figure 3. The X-ray diffraction (XRD) spectra of the synthesized graphene foam are provided in Figure 3f. Note that the observation of possible carbon particles in Figure 3b is the result of Ni etching, where part of the graphene layer was affected by a little defect. Therefore, we confirm the presence of graphene by XRD, TEM, and Raman.

2.2. Electrochemical Preparation and Measurements. Electrochemical experiments employed a three-electrode cell featuring a platinum-wire counter electrode, Ag/AgCl (with 3 M KCl inner solution) as the reference electrode, and NGAL antibodies immobilized on a GF/Ni working electrode (Figure 2). The cyclic voltammetry (CV) was conducted under a 50 mV/s scan rate in the presence of ferri/ferrocyanide redox in 0.1 M KCl with the potential ranging from 0.0 to 0.8 V in NGAL solutions with various concentrations of 2.7−140 ng/mL with pH 7.2 phosphate buffer solution (PBS). Palmsens 2 potentiostat was used as an electrochemical analyzer with PSTrace 1.4 software. After oxidation potential was found from CV, the potential was further picked up for amperometry. For quantitative measurements, 0.2 mL of a human urine sample with known NGAL concentration was sequentially added to identify the potential at which oxidation peaks occurred. In chronoamperometry, we recorded current responses following consecutive NGAL additions to the electrochemical system, starting at an onset potential of 0.4 V. These results were compared to conventional ELISA measurements .

The electrochemical determination is based on cyclic voltammetry (CV) and chronoamperometry using our developed enzymatic microporous graphene electrode. CV was carried out with a 50 mV/s scan rate in buffer solutions (PBS; pH = 7.2). We conducted CV to determine the oxidation potential, which was then picked up and used in amperometry. Once the oxidation potential was determined, we picked up the potential to be fixed for chronoamperometry. In amperometry, we subsequently dropped urine with specific NGAL concentrations and waited for a steady current before the next drop. Results and correlation between concentrations and currents are reported in the next section.

2.3. Chemicals, Materials, and Instrumentation. The process used to fabricate the graphene/nickel foam was similar to the method described in the previous study.[15] The NGAL antibody (Anti-LCN2) and lipocalin-2 were obtained from Sigma-Aldrich (Missouri) and SinoBiological (Beijing, China), respectively. The human lipocalin-2/NGAL ELISA kit was purchased from Sigma-Aldrich (Missouri), and the analytical-grade deionized water (DI) and phosphate-buffered solution (PBS) were prepared by the Department of Biochemistry at Khon Kaen University. Graphene/Ni foam functionalized with the NGAL antibody was used as the transducer electrode.

2.4. NGAL Antibody Addition. GF prepared from CVD will be functionalized with NGAL antibody (Anti-LCN2) via carboxyl group functionalization. In the oxidation process, we applied sulfuric acid (1 M H_2SO_4) as the oxidizing agent to GF at 35 °C. For the postoxidation process, we diluted and washed the mixture with deionized water to remove excess acids and byproducts, followed by centrifugation to separate the oxidized graphene and then drying in a vacuum oven. NGAL antibodies were conjugated to the carboxyl groups using 4 μg/L EDC (1-ethyl-3-(3-(dimethylamino)propyl)carbodiimide) and 6 μg/L NHS (*N*-hydroxysuccinimide), creating stable amide bonds.

https://doi.org/10.1021/acsomega.4c01315
ACS Omega 2024, 9, 21276−21286

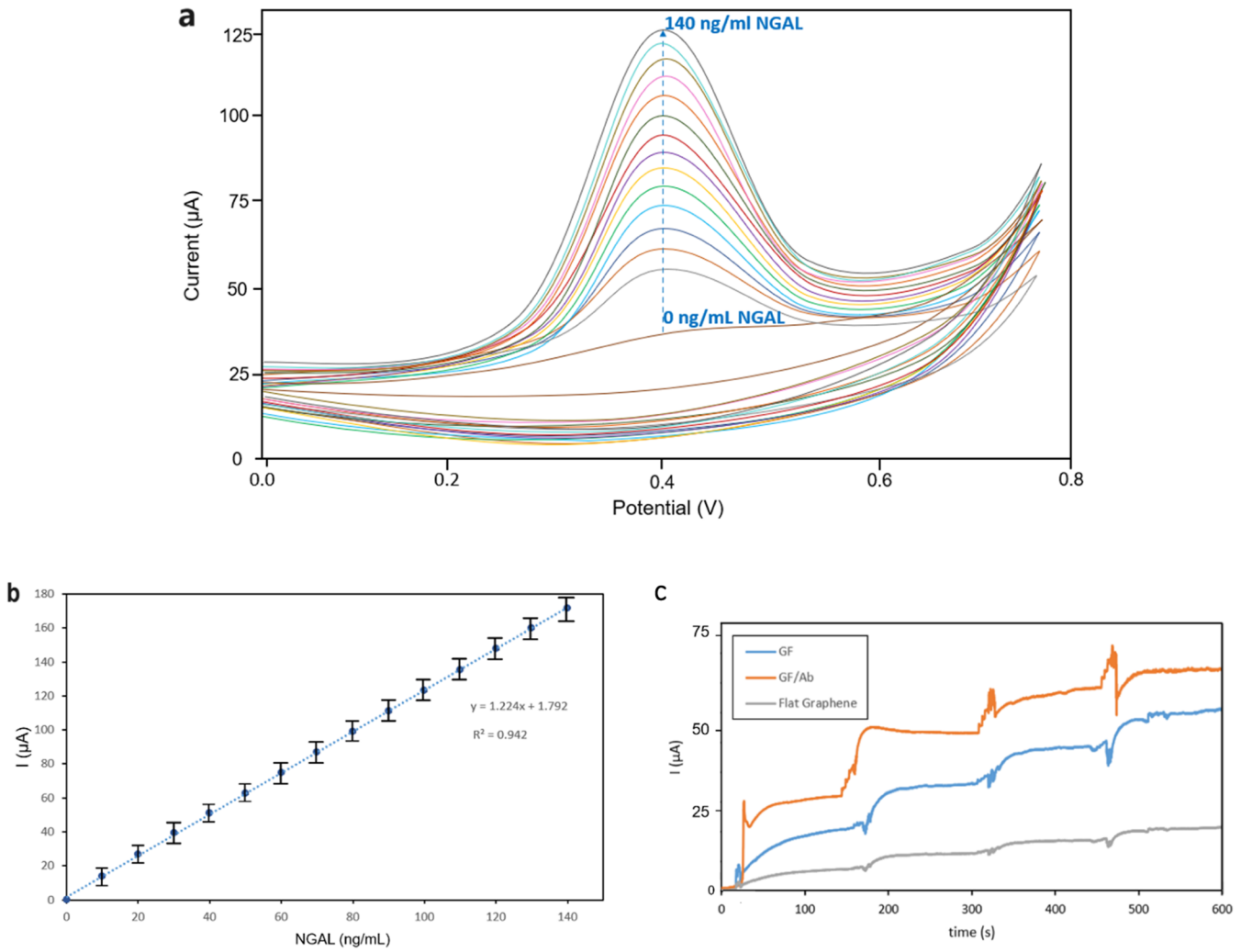

Figure 5. (a) Results of studying the electrical potential using cyclic voltammetry on NGAL within 0.2 M PBS (pH = 7.2) solution with 50 mVs^{-1} scan rate and five cycles of running were averaged for each concentration. (a) CV over various concentrations of NGAL from 0, 10, 20, 30, ⋯, 140 ng/mL. (b) Linear plot of CV current vs NGAL concentrations. (c) Chronoamperometry comparing GF/Ni (orange), GF/Ni/Anti-LCN2 (blue) working electrode, and flat graphene electrode (gray).

Raman spectroscopy was collected for GF before and after the addition of carboxyl groups and Anti-LCN2 to verify the carboxyl group functionalization. There were characteristic peaks of carboxyl groups and antibodies added to ordinary graphene peaks (Figure 3e).

2.5. Machine Learning Models. Since the electrolytes and proteins were found to partially interfere with the NGAL detection, we introduce machine learning models to exclude the contribution of interference and improve detection accuracy. Machine learning models for regression in this study include support vector machines (SVMs), multilayer perceptrons (MLPs), random forests (RFs), and extreme learning machines (ELMs). SVM identifies a hyperplane for linear or nonlinear relationships with a balance between complexity and performance. MLP can capture complex relationships with an adaptable architecture. RF combines decision trees for robust predictions and feature importance assessment. ELM merits AUC performance and model simplicity due to computational efficiency, shallow architecture, and regularization options. Performance comparison will be reported and discussed in the next section.

2.6. Extreme Learning Machine. Extreme learning machine (ELM) has gained much attention due to its simplicity compared to attainable performance as well as several advantages: (i) exceptional computational efficiency, making it ideal for large data sets and time-sensitive applications; (ii) simplicity and ease of implementation, which allows for straightforward model setup and reduced expertise requirements; (iii) a shallow architecture with a single hidden layer that mitigates overfitting concerns, improving AUC performance by reducing complexity; (iv) strong generalization capabilities that enable ELM to capture complex, nonlinear data relationships, enhancing AUC scores; and (v) ability to incorporate regularization techniques like ridge regression, further fine-tuning the model's performance and balancing complexity with AUC performance. These characteristics make ELM a powerful and accessible option for regression tasks.

In an ELM algorithm, a training set γ is defined by Huang et al.[17]

$$\gamma = \{(x_i, t_i) | x_i \in \boldsymbol{R}^n, t_i \in \boldsymbol{R}, i = 1, 2, 3, ..., N\}$$

The prediction value y_i is given by

https://doi.org/10.1021/acsomega.4c01315
ACS Omega 2024, 9, 21276−21286

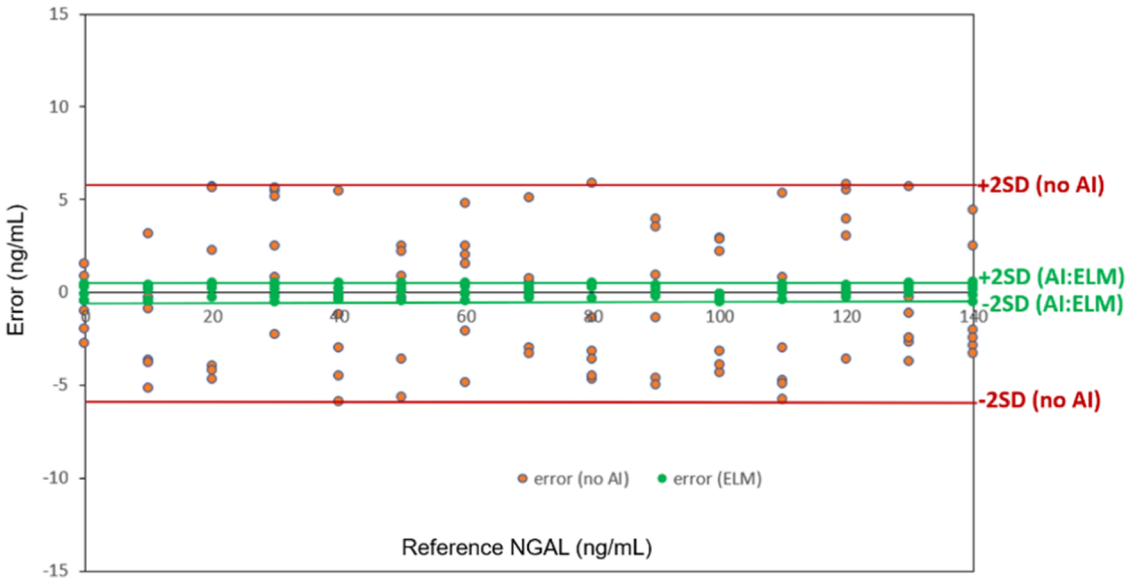

Figure 6. Bland–Altman plot of the pure electrochemical method (orange) and hybrid extreme learning machine (ELM) with an electrochemical measure (green).

$$y_i = \sum_{j=1}^{M} \beta_j g(w_j \cdot x_i + b_j)$$

where x_i is the ith sample data or $x_i = [x_{i1}, x_{i2}, \cdots, x_{iN}]^T \in \boldsymbol{R}^n$, target t_i is a target scalar of the weight $w_j = [w_{i1}, w_{i2}, \cdots, w_{iN}]^T$; j = 1, 2, ⋯, M, n is the feature dimension, in our study n = 5 (Figure 4), and activation function $g(x)$ is defined by sigmoid function or $g(x) = \frac{1}{1+e^{-x}}$. M is the number of hidden nodes and N is the number of samples. The ELM algorithm can be divided into the following steps:

Step 1: Randomize weight w_j and bias b_j, where j = 1,2,3, ⋯, M.

Step 2: Compute the hidden layer matrix **H**.

H is an N × M matrix defined by its elements as[17]

$$\mathbf{H}_{ij} = g(w_j \cdot x_i + b_j)$$

Step 3: Calculate the output weight $\boldsymbol{\beta}$ by

$$\boldsymbol{\beta} = \mathbf{H}^{\dagger}\mathrm{T}$$

where $\mathbf{H}^{\dagger}$ is the Moore–Penrose generalized inverse of **H**,i.e.,

$$\mathbf{H}^{\dagger} = (\mathbf{H}^{\mathrm{T}}\mathbf{H})^{-1}\mathbf{H}^{\mathrm{T}}$$

Note that $\mathbf{T} = [t_1, t_2, ..., t_N]^T$ is the target vector carrying reference NGAL values of N samples.

The overall result is the predicted outcome y representing the model's output or predicted NGAL based on the input (amperometric current, electrolytes, and albumin). Results show that ELM (Figure 4) yields the greatest performance in terms of AUC (Figure 7).

2.7. Subjects and Specimens. The study was approved by the Center for Ethics in Human Research at Khon Kaen University Ethics Committee for Human Research (HE 641098). Informed consent was obtained from all subjects and their legal guardian(s). All experiments were performed in accordance with the relevant guidelines and regulations approved by the committee. The specimens involved 135 urine samples (Tables 1 and 2), initially frozen at −20 °C and later thawed at 4 °C for examination.

3. RESULTS

3.1. Electrochemical Sensing Characteristics. *3.1.1. Cyclic Voltammogram.* We carried out CV over the PBS solution with varying NGAL concentrations from 0 up to 140 ng/mL and determined the oxidation potential where the current yields the greatest response to the NGAL concentrations. Using a 50 mV/s scan rate, the oxidation potential

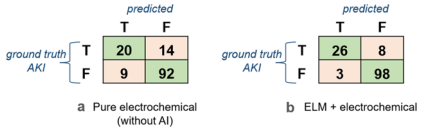

Figure 7. Confusion matrices of AKI prediction for (a) pure GF/Ni/Anti-LCN2 electrochemical determination. (b) ELM + electrochemical sensing. AKI cutoff was set at 100 ng/mL in this evaluation.

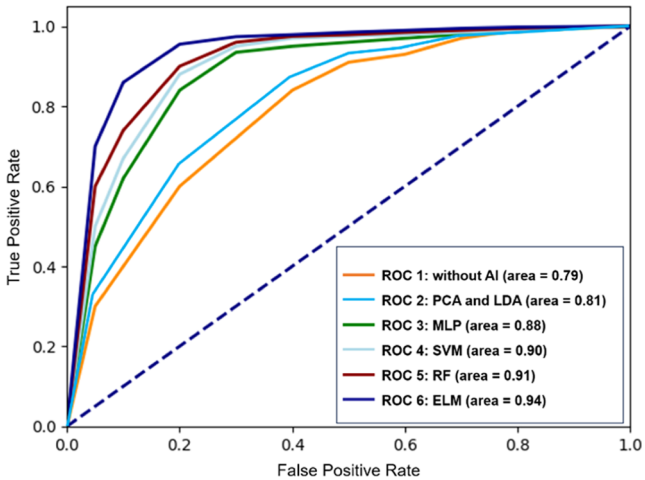

Figure 8. ROC curves of (i) pure electrochemical measurement (orange) and with augmented ELM to the electrochemical measure (dark blue) show an AUC improvement from 0.79 (without AI) to 0.81 (PCA + LDA) 0.88 (MLP), 0.90 (SVM), 0.91 (RF), and 0.94 (ELM).

https://doi.org/10.1021/acsomega.4c01315
ACS Omega 2024, 9, 21276−21286

Table 3. Comparison of Performances of Different Chemometrics[a]

methods	accuracy	precision	sensitivity	specificity	F1 score
without AI	0.83	0.59	0.69	0.87	0.63
PCA + LDA	0.85	0.63	0.76	0.88	0.69
MLP	0.87	0.70	0.77	0.90	0.73
SVM	0.89	0.73	0.80	0.91	0.76
RF	0.90	0.74	0.83	0.91	0.78
ELM	0.92	0.90	0.76	0.97	0.82

[a]ELM achieved a performance of 92% accuracy, 90% precision, 76% sensitivity, 97% specificity, and 82% F1 score. Without a machine learning model, the performance achieved was 83% accuracy, 59% precision, 69% sensitivity, 87% specificity, and 63% F1 score.

was found to be 0.4 V (Figure 5a). This potential will be picked up and fixed in later chronoamperometry. The buffer solutions, pH, and other configurations were kept constant to ensure that the oxidation potential level did not differ in the following amperometry.

3.1.2. Amperometry. In chronoamperometry, we compared GF/Ni and GF/Ni/Anti-LCN2 antibody working electrodes at an oxidation peak potential of 0.4 V. We observed the current response according to increasing NGAL concentrations in a buffered solution of 5 mL. We dropped 0.2 mL of urine containing 0.5 μg/mL NGAL, which yielded 20 ng/mL NGAL in 5 mL of the PBS (pH = 7.2) solution. Each drop, which was attributed to 20 ng/mL NGAL within the solution, led to current increments of 26.4 ± 7.34 μA per step, with a rapid response within 20 s. The standard deviation of the measured current was 3.67 μA. SD and errors (2SD) will be improved after introducing ELM (next subsections). Throughout all four steps, GF/Ni/Anti-LCN2 samples consistently showed higher current values than GF/Ni, except for the final step, where the current response declined due to antigen depletion in GF/Ni/Anti-LCN2 samples. Statistical analysis, including Kolmogorov−Smirnov and *t* tests, confirmed a normal distribution and significant differentiation between samples (*t* stat > *t* critical, *p*-value <0.05). The electrochemical sensor incorporating ELM displayed markedly improved precision, reducing SD, compared to bare GF/Ni/Anti-LCN2.

3.1.3. Calibration Curve. A calibration curve showed the relationship between the amperometric method's current and the NGAL levels measured by ELISA. The LR of 2.7−140 ng/mL was calculated using a correlation coefficient of 0.942 without AI and 0.986 with ELM (Figure 6a). With ELM incorporated with the GF/Ni/Anti-LCN2 electrode, the limit of detection (LOD) for NGAL was calculated as 0.89 ng/mL (with ELM) (14.8 ng/mL without ELM). The limits of quantitation (LOQ) were 2.7 (with ELM) and 44.8 ng/mL (without ELM). Note that LOD = $\frac{3.3\cdot SD}{slope}$ and LOQ = $\frac{10\cdot SD}{slope}$ where SD (with ELM) = 0.27 ng/mL = 0.33 μA, SD (without ELM) = 3 ng/mL = 3.67 μA, and slope = 1/1.224 (μA × mL/ng).

3.1.4. Statistics. Statistical testing with the Bland−Altman plot revealed that the relationship and difference between the measurement and actual data were in good agreement. It was found that, at 95% confidence, the error is between ±0.54 ng/mL (for AI-empowered methods) and ±6 ng/mL (without AI methods), where the cutoff for AKI is approximately 100 ng/mL depending on patients' conditions (Figure 6). These experiments were collected with amperometric determination mode, for it will be further developed as a fixed-potential small sensing device.

To determine the AKI prediction performance in terms of precision, accuracy, and specificity, we have to fix the NGAL cutoff value for AKI; 100 ng/mL was used in this case. The confusion matrices of AKI diagnosis using pure electrochemical and ELM empowering prediction are shown below.

According to Figure 7a, pure electrochemical AKI prediction yields 82.96% accuracy, 68.97% precision, 91.09% specificity, and 63.43% F1 score. Meanwhile, in Figure 7b, the ELM-empowered electrochemical method showed 91.85% accuracy, 89.66% precision, 97.03% specificity, and 82.54% F1 score. These showed significant improvement after adding ELM to the AKI prediction, where accuracy, precision, sensitivity, specificity, and F1 score all significantly increased by 8.89, 30.69, 6.78, 9.94, and 19.07%, respectively.

Table 4. Electrochemical Immunosensor Reported for the Determination of NGAL[a,b]

electrode	transduction technique	L.R. (ng/mL)	LOD (ng/mL)	sample	ref
ITO/TiO2/CoPc/CS/SA/BSA/BiNb/NGAL photoelectron-chemical sensor	PEC	1.0−500.0 pg/mL	0.6 pg/mL	serum	Li et al.[12]
GSPE/P(ATT)-GO/AuNPs/Apt1/LCN2/Apt2	DPV	1.0−1,000.0	0.3	fetal bovine serum	Tığ et al.[13]
carbon/enzyme-based sandwiches	CV	0.15−2	97 pg/mL	urine	Neves et al.[14]
GF/AuNPs/SAM/immunosensor	CV and amperometric	0.05−210.0	0.042	urine	Danvirutai et al.[15]
aniline functionalized G/PANI nanodroplet-modified electrode	CV and DPV	50.0−500.0	21.1	urine	Yukird et al.[18]
LA2/AuNPs/PAMAM modified gold electrode	CV and amperometric	50.0−250.0	1.0	serum and urine	Kannan et al.[19]
affinity peptide-incorporated	CV and EIS	1.0−100.0	1.74	serum	Cho et al.[20]
BCN/immunosensor	CV and EIS	0.001−10	0.37 pg/mL	serum	Chen et al.[21]
GF/Ni/Anti-LCN2 + ELM	CV and amperometric	2.7−140	0.89	urine	this work

[a]CV: cyclic voltammograms; DPV: differential pulse voltammetry; G: graphene; PANI: polyaniline; LA2: rabbit polygonal lipocalin-2 antibody; AuNPs: gold nanoparticles; PAMAM: generation-1 polyamidoamine; NGAL: neutrophil gelatinase-associated lipocalin; P(ATT)-GO: poly-3-amino-1,2,4-triazole-5-thiol/graphene oxide composite; GSPE: graphite screen-printed electrode; LCN2: lipocalin-2; APT 1: thiol-tethered DNA aptamer; APT2: biotinylated secondary aptamer; SAM: self-assembled-monolayer; ITO: indium tin oxide, TIO_2: titanium dioxide; COPC: streptavidin-coated cobalt 2,9,16,23-tetraaminophthalocyanine; CS: chitosan; SA: streptavidin; BSA: bovine serum albumin; PEC: photo-electrochemical; EIS: electrochemical impedance spectroscopy. [b]Adapted from Sittihakote et al.[22]

https://doi.org/10.1021/acsomega.4c01315
ACS Omega 2024, 9, 21276−21286

Table 5. Comparison of Machine Learning Contributions to Kidney Biomarker Detection in the Literature[a]

sensing materials/methods	data set	ML target	ML model	improvement (against w/o AI)	merits	drawbacks	ref
standard invasive blood serum determinations of various parameters except creatinine	serum determinations: HbA1C, K^+, Cl^-, Na^+, cholesterol, HDL, LDL, bilirubin, uric acid, etc.	creatinine	ensemble learning models	claimed 100% accuracy (loads of data required)	reports a large number of correlations. found vitamin D contributions to creatinine	costs in determinations of large information in serum invasive creatinine prediction does not cover real-time AKI diagnosis but represents 72 h in the past	Haratian et al.[23]
standard invasive blood serum determinations of various parameters except creatinine	RONS image, NGAL, GGT, KIM-1, and miRNA21	AKI diagnosis	linear regression, generalized additive model, decision tree, SVMs, logistic regression, gradient-boosted decision tree		concluded that plenty of research is still is need of improvement of AKI prediction	no comparison to the advanced algorithm, e.g., XGBoost, LightGBM	Xiao et al.[16]
microporous graphene with anti-LCN2 coated	NGAL-correlated amperometric current, Na^+, Cl^-, K^+, albumin, and proteins	NGAL	ELM	AUC increases by 15%	fast and accurate	N/A	this work

[a]HbA1C: glycated hemoglobin A1C; K^+: potassium ions; Cl^-: chloride ions; Na^+: sodium ions; HDL: high-density lipoprotein; LDL: low-density lipoprotein; RONS: reactive oxygen and nitrogen species; GGT: γ-glutamyl transferase; Kim-1: kidney injury molecule-1; miRNA21: micro-RNA 21; RNNs: recurrent neural networks; XGBoost: extreme gradient-boosting algorithm; LightGBM: light gradient-boosting machine.

3.1.5. Chemometrics for AKI Prediction: Performance Comparison between Pure Electrochemical vs Machine Learning Assisted. To estimate the performance of AKI prediction, the cutoff urine NGAL level was assumed to be fixed at 100 ng/mL. In this work, using the pure electrochemical method for AKI diagnosis, we achieve an AUC of 0.79. After embedding ELM for further accuracy improvements, the AUC increased to 0.94, as shown in the ROC curve in Figure 8. Introducing ELM, a minimal machine learning algorithm, to the model could improve the performance by about 15%. The result found that ELM yielded the greatest performance compared to other machine learning algorithms (Figure 8). Since principal component analysis (PCA) and linear discriminant analysis (LDA) suit the linear model, which is not the case of multiple interferences, the PCA + LDA performance lies below those of other ML methods. The performance in terms of accuracy, precision, sensitivity, specificity, and F1 score is compared in Table 3, with the AKI cutoff level set at 100 ng/mL.

3.1.6. Comparison with Previous Studies. The study compared it to prior research on measuring the NGAL concentration using an electric current in an electrode. Most of the prior research focused on modifications to increase the detection efficiency and various transduction techniques based on the electrochemical immunosensor's concepts (Table 4). The linear range and LOD were used to determine that the previous study necessitated complex preparation steps and a long analytical period. Neves et al. (2019) used carbon/enzyme-based sandwiches electrode for ultralow LOD (97 pg/mL); however, it spans a very narrow linear range (0.15−2 ng/mL), which does not cover the AKI cutoff value and would involve steps of urine dilutions and back calculations. In our work, the linear range covers the AKI cutoff decision around 100 ng/mL with acceptable LOD. In contrast to a number of literature using synthetic urine, which does not involve unknown interference sources in human urine, our work measures the actual human urine samples. The numerous electrolytes, proteins, and substances in real urine do contribute to the specificity and performance of the sensor to a certain level that limits the performance of pure electrochemical sensing. To resolve interferences from various chemical species in urine, machine learning via ELM was introduced in this work, and the performance was reported. Machine-learning-contributed AKI diagnosis studies are summarized in Tables 3 and 5 and Figure 8.

In Table 5, the literature mainly focuses on the prediction of AKI directly from large parameters of serum, which is considered to be expensive. Another approach attempted to predict serum creatinine (SCr) from multiple urine parameters. SCr represents the kidney injury status of 72 h in the past, not real time. Machine learning's assistance to the electrochemical determination of NGAL is still missing in the literature, which will be filled up in this work.

3.2. AKI Prediction Performance Using Extreme Learning Machine. Human urine contains several electrolytes that could affect the conductivity and, thus, the intensity of the amperometric current readout. The electrolytes included sodium (Na+), potassium (K+), and chloride (Cl-). We stress that the interference of these electrolytes could be significantly removed by applying an extreme learning machine (ELM) to the regression model. The combined ELM and current readout could improve the overall performance (AUC, accuracy, precision, specificity, and F1 score). Assuming the AKI cutoff

https://doi.org/10.1021/acsomega.4c01315
ACS Omega 2024, 9, 21276−21286

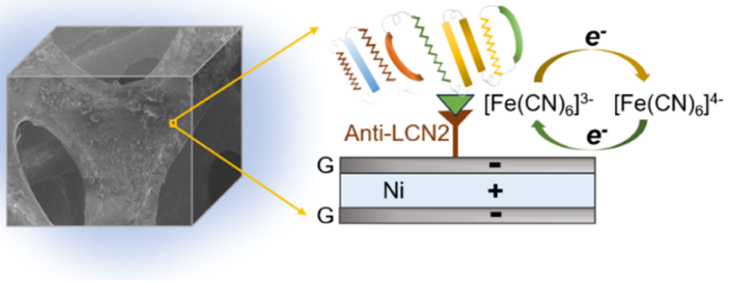

Figure 9. Mechanism of action: redox occurs via ferrous/ferrocyanide mediators exchanging electrons and yielding current at the electrode. NGAL antibody (anti-LCN2) was functionalized at the surface to selectively bind with NGAL protein. Graphene−nickel dipole−dipole enhancement improves the electrode's sensitivity.

at 100 ng/mL, ELM could improve the performance in terms of AUC by 15%. ROC curves of different machine learning models were compared, and ELM yielded the best. In addition, the Bland−Altman plots showed an improvement in errors from 6 to 0.54 ng/mL using ELM.

Figure 2 illustrates the step of training the ELM and contains the data records of urine including current (μA), Cl^-, Na^+, K^+, protein, and microalbumin. These might be interferences with electrochemical sensing. On the other hand, it can be used as additional information to train neural networks for further accuracy improvement. In our ELM implementation, single dense layers with 50 nodes were used. Sigmoid functions were used in the hidden layer. Rectified linear unit (ReLU) was used as the last activation function to numerically predict the NGAL level. Results showed that AUC increased by 15% after introducing ELM to the amperometry.[24]

4. DISCUSSION

A three-electrode system was set up, where GF/Ni/Anti-LCN2 was put as the active electrode. Cyclic voltammetry (CV) was conducted to determine the oxidation potential. Under the fixed applied potential found from CV, chronoamperometry was carried out to take correlation statistics between the amperometric response and the NGAL concentration. This research reveals the viability of a 3D GF/Ni enzymatic electrochemical sensor for the detection of NGAL in actual human urine using ELM for enhancing AKI prediction performance. The integration of ELM into the AKI prediction method markedly enhanced the performance metrics, resulting in substantial increases of 8.89% in accuracy, 30.69% in precision, 6.78% in sensitivity, 9.94% specificity, and 19.07% in the F1 score.

Figure 9 illustrates the mechanism of the current response to each NGAL adsorption. The current from NGAL flowed through the [Fe(CN6)]3-/[Fe(CN6)]4- mediator and enhanced the reactive signal via dipole−dipole enhancement (Zhang, 2018). The GF/Ni/Anti-LCN2 electrode with ELM displayed the ability to detect NGAL concentrations, with a linear range of 2.7−140 ng/mL, a limit of detection of 0.89 ng/mL, and a limit of quantitation of 2.67 ng/mL. The study on specificity found that between creatinine (Cr), protein, urine microalbumin, sodium (Na), potassium (K), and chlorine (Cl), none of the tested substances interfered with NGAL detection and that NGAL can be measured in human urine with good % recoveries (85.69−111.67%) and precision or reproducibility (%RSD = 8.54%). Importantly, NGAL levels in urine samples from AKI patients measured by this system are in good agreement with the outcomes of a standard ELISA method, while our system has simpler fabrication processes, is rapid (1−2 min total time assay), is user-friendly (hands-on time <10 min), requires fewer samples (0.2 mL), and especially has a lower operating cost. This biosensor can be viewed as a significant development toward noninvasive early-stage AKI diagnosis by analyzing urine samples because it is affordable, specific, and extremely sensitive. To improve selectivity and lower the LOD, previous research suggested using antibody immobilization on the working electrode with enzymes for improved stability. Adding neural networks to the amperometric detection can improve the performance by a 15% AUC increment over the non-AI method. According to the Bland−Altman plots, the error was improved from ±6 ng/mL (without ELM) down to 0.54 ng/mL (with ELM). For comparison of the contributions of different ML models to AKI prediction performance, the cutoff level of urine NGAL was fixed at 100 ng/mL. ELM was compared with MLP, SVM, and RF. ELM showed the best AUC, precision, and accuracy performances. Although the NGAL cutoff level for AKI can vary depending on the age, cause of kidney injury, and timing of sample collection relative to the suspected injury, it is assumed to be constant for comparison of NGAL determination and AKI prediction using different ML models. For a clinical decision, nephrologists need to determine the NGAL level with the overall patient's condition. A limitation of this approach is the necessity for supplementary urine data to train the ELM. If available urine parameters are fewer than those used in this study, the ELM is still capable of making accurate predictions with reduced features, potentially augmenting the efficacy of pure electric current determination. This work reports the first use of a graphene-based electrode integrated with the ELM network to enhance the electrochemical determination of urine NGAL for AKI diagnosis.

5. CONCLUSIONS

This study demonstrates the incorporation of a 3D graphene microporous immunoassay (GF/Ni/Anti-LCN2) electrode with an extreme learning machine (ELM) to improve the detection of gelatinase-associated lipocalin (NGAL) in urine, which is an early indicator of acute kidney injury (AKI). The combination of GF/Ni/Anti-LCN2 and ELM increased the area under the curve (AUC) by 15%, reduced mean absolute errors by 5.44 ng/mL (from 6 to 0.54 ng/mL), and reduced the limit of detection to 0.89 ng/mL (from 44.8 ng/mL). The addition of ELM for AKI prediction significantly improved performance metrics, increasing accuracy from 82.96 to 91.85%, precision from 58.97 to 89.66%, sensitivity from 69.42 to 76.20%, specificity from 87.09 to 97.03%, and F1

https://doi.org/10.1021/acsomega.4c01315
ACS Omega 2024, 9, 21276−21286

score from 63.43 to 82.50%, enhancements of 8.89, 30.69, 6.78, 9.94, and 19.07%, respectively. For a fixed threshold of AKI using the NGAL biomarker, the prediction performance showed significant improvement in terms of accuracy, precision, and specificity. The work could be a candidate tool for clinical diagnostics of AKI that is simple, cheap, and highly accurate compared to the other work. Future work should extend the results from the laboratory scale to clinical implementations of the device.

■ ASSOCIATED CONTENT

Data Availability Statement

The data sets generated and/or analyzed during the current study are not publicly available due to ethical reasons involving personal confidentiality but are available from the corresponding author upon reasonable request.

■ AUTHOR INFORMATION

Corresponding Author

Chavis Srichan − *Faculty of Engineering, Biomedical Engineering, Khon Kaen University, Nai Mueang 40002 Khon Kaen, Thailand; Faculty of Engineering, Computer Engineering, Khon Kaen University, Nai Mueang 40002 Khon Kaen, Thailand;* orcid.org/0000-0002-4772-3543; Email: chavis@kku.ac.th

Authors

Netnapa Sittihakote − *Faculty of Engineering, Biomedical Engineering, Khon Kaen University, Nai Mueang 40002 Khon Kaen, Thailand*

Pobporn Danvirutai − *Faculty of Engineering, Computer Engineering, Khon Kaen University, Nai Mueang 40002 Khon Kaen, Thailand*

Sirirat Anutrakulchai − *Faculty of Medicine, Khon Kaen University, Nai Mueang 40002 Khon Kaen, Thailand; Chronic Kidney Disease Prevention in the Northeast of Thailand, Khon Kaen University, Nai Mueang 40002 Khon Kaen, Thailand*

Adisorn Tuantranont − *National Science and Technology Development Agency, Khlong Luang 12120 Pathum Thani, Thailand*

Complete contact information is available at: https://pubs.acs.org/10.1021/acsomega.4c01315

Author Contributions

N.S. and P.D. performed the formal analysis and methodology and wrote the original draft. S.A. was responsible for formal analysis, data curation, and validation. A.T. was responsible for the methodology and supervision. C.S. performed the formal analysis and was responsible for methodology, writing the original draft, and reviewing and editing the manuscript.

Notes

The authors declare no competing financial interest.

■ ACKNOWLEDGMENTS

This research was supported by the Chronic Kidney Disease in Northeast Thailand (CKDNET), the Biomedical Engineering Department at Khon Kaen University, and the National Science and Technology Development Agency (NSTDA). This work was funded by Thailand Science Research and Innovation (TSRI) through Program Management Unit for Competitiveness (PMUC), contract number C10F630030.

■ REFERENCES

(1) Kellum, J. A.; Romagnani, P.; Ashuntantang, G.; Ronco, C.; Zarbock, A.; Anders, H.-J. Acute kidney injury. *Nat. Rev. Dis. Primers* **2021**, *7* (52), 1−7.

(2) Yi, A.; Lee, C.-H.; Yun, Y. M.; Kim, H.; Moon, H.-W.; Hur, M. Effectiveness of Plasma and Urine Neutrophil Gelatinase-Associated Lipocalin for Predicting Acute Kidney Injury in High-Risk Patients. *Ann. Lab. Med.* **2017**, *41*, 60−67.

(3) Mårtensson, J.; Bellomo, R. The Rise and Fall of NGAL in Acute Kidney Injury. *Blood Purif.* **2014**, *3*, 304−310.

(4) Malyszko, J.; Lukaszyk, E.; Glowinska, I.; Durlik, M. Biomarkers of delayed graft function as a form of acute kidney injury in kidney transplantation. *Sci. Rep.* **2015**, *5*, No. 11684.

(5) Schrezenmeier, E. V.; Barasch, J.; Budde, K.; Westhoff, T.; Schmidt-Ott, K. M. Biomarkers in acute kidney injury − pathophysiological basis and clinical performance. *Acta Physiol.* **2017**, *219*, 554−572.

(6) Kellum, J. A.; Lameire, N. Diagnosis, evaluation, and management of acute kidney injury: a KDIGO summary (Part 1). *Crit. Care* **2013**, *17*, 204.

(7) Mercado, M. G.; Smith, D. K.; Guard, E. L. Acute Kidney Injury: Diagnosis and Management. *Am. Fam Physician* **2019**, *100* (11), 687−694. PMID: 31790176

(8) McIlroy, D. R.; Wagener, G.; Lee, H. T.; Riou, B. Biomarkers of acute kidney injury: an evolving domain. *J Am Soc Anesthesiol.* **2010**, *112* (4), 998−1004.

(9) Rysz, J.; Gluba-Brzózka, A.; Franczyk, B.; Jabłonowski, Z.; Ciałkowska-Rysz, A. Novel Biomarkers in the Diagnosis of Chronic Kidney Disease and the Prediction of Its Outcome. *Int. J. Mol. Sci.* **2017**, *18*, 1702.

(10) Wagener, G.; Jan, M.; Kim, M.; Mori, K.; Barasch, J. M.; Sladen, R. N.; Lee, H. T. Association between Increases in Urinary Neutrophil Gelatinase−associated Lipocalin and Acute Renal Dysfunction after Adult Cardiac Surgery. *Anesthesiologists* **2006**, *105*, 485−491.

(11) Krzeminska, E.; Wyczalkowska-Tomasik, A.; Korytowska, N.; Paczek, L. Comparison of Two Methods for Determination of NGAL Levels in Urine: ELISA an CMIA. *J. Clin. Lab. Anal.* **2016**, *30*, 956−960.

(12) Li, H.; Mu, Y.; Yan, J.; Cui, D.; Ou, W.; Wan, Y.; Liu, S. Label-Free Photoelectrochemical Immunosensor for Neutrophil Gelatinase-Associated Lipocalin Based on the Use of Nanobodies. *Anal. Chem.* **2015**, *87* (3), 2007−2015.

(13) Tığ, G. A.; Pekyardımcı, Ş. An electrochemical sandwich-type aptasensor for determination of lipocalin-2 based on graphene oxide/polymer composite and gold nanoparticles. *Talanta* **2020**, *210*, No. 120666.

(14) Neves, M. M. P. S.; Nouws, H. P. A.; Santos-Silva, A.; Delerue-Matos, C. Neutrophil gelatinase-associated lipocalin detection using a sensitive electrochemical immunosensing approach. *Sens. Actuators, B* **2020**, *304*, No. 127285.

(15) Danvirutai, P. M.; Ekpanyapong, M.; Tuantranont, A.; Bohez, E.; Anutrakulchai, S.; Wisitsoraat, A.; Srichan, C. Ultra-sensitive and label-free neutrophil gelatinase-associated lipocalin electrochemical sensor using gold nanoparticles decorated 3D Graphene foam towards acute kidney injury detection. *Sens. Bio-Sens. Res.* **2020**, *30*, No. 100380.

(16) Xiao, Z.; Huang, Q.; Yang, Y.; Liu, M.; Chen, Q.; Huang, J.; Xiang, Y.; Long, X.; Zhao, T.; Wang, X.; Zhu, X.; Tu, S.; Ai, K. Emerging early diagnostic methods for acute kidney injury. *Theranostics* **2022**, *12* (6), 2963−2986.

(17) Huang, G.-B.; Zhu, Q.-Y.; Siew, C.-K. Extreme learning machine: Theory and applications. *Neurocomputing* **2006**, *70* (1−3), 489−501.

(18) Yukird, J.; Wongtangprasert, T.; Rangkupan, R.; Chailapakul, O.; Pisitkun, T.; Rodthongkum, N. Label-free immunosensor based on graphene/polyaniline nanocomposite for neutrophil gelatinase-associated lipocalin detection. *Biosens. Bioelectron.* **2017**, *87*, 249−255.

(19) Kannan, P.; Tiong, H. Y.; Kim, D.-H. Highly sensitive electrochemical determination of neutrophil gelatinase-associated lipocalin for acute kidney injury. *Biosens. Bioelectron.* **2012**, *31*, 32−36.
(20) Cho, C. H.; Kim, J. H.; Song, D.-K.; Park, T. J.; Park, J. P. An affinity peptide-incorporated electrochemical biosensor for the detection of neutrophil gelatinase-associated lipocalin. *Biosens. Bioelectron.* **2019**, *142*, No. 111482.
(21) Chen, Z.; Lu, M. Thionine-coordinated BCN nanosheets for electrochemical enzyme immunoassay of lipocalin-2 on biofunctionalized carbon-fiber microelectrode. *Sens. Actuators, B* **2018**, *304*, 253−259.
(22) Sittihakote, N.; Anutrakulchai, S.; Tuantranont, A.; Danvirutai, P.; Srichan, C. *Acute Kidney Injury Detection using Real Human Urine NGAL Biomarker Sensor based on 3D Graphene*, Proceedings of the 14th Biomedical Engineering International Conference (BMEiCON): Songkhla, Thailand, 2022; pp 1−4 DOI: 10.1109/BMEiCON56653.2022.10012085.
(23) Haratian, A.; Maleki, Z.; Shayegh, F.; et al. Detection of factors affecting kidney function using machine learning methods. *Sci. Rep.* **2022**, *12*, No. 21740.
(24) Xuan, X.; Hossain, M.; Park, J. A Fully Integrated and Miniaturized Heavy-metal-detection Sensor Based on Micropatterned Reduced Graphene Oxide. *Sci. Rep.* **2016**, *6*, No. 33125.

https://doi.org/10.1021/acsomega.4c01315
ACS Omega 2024, 9, 21276−21286